Jonathan Huang was born in New Brunswick, NJ and grew up in Princeton. He attended Dartmouth College, double-majoring in math and physics. During his undergraduate career, he held two SULI internships at the Princeton Plasma Physics Laboratory in the winter and summer of 2005. He hopes to enter a PhD program in mathematics and become a professor. His interests include chess and ultimate frisbee.

Jon Menard, Princeton Plasma Physics Laboratory (PPPL), received the Presidential Early Career Award for Scientists and Engineers. He is an experimental plasma physicist who works primarily on the National Spherical Torus Experiment (NSTX) at PPPL. Dr. Menard's research interests include the linear and non-linear magnetohydrodynamic (MHD) stability properties of spherical torus (ST) plasmas, advanced operating scenarios in the ST, plasma startup, and high-harmonic fast wave physics, and performing studies to optimize the stability of fusion plasmas and providing the heart of the physics basis for a new, spherical plasma fusion reactor. After receiving a bachelor's degree in nuclear engineering from the University of Wisconsin-Madison in 1992, Dr. Menard went on to receive a master's and a Ph.D. in plasma physics from Princeton University, Department of Astrophysical Sciences, in 1994 and 1998, respectively. He conducted post-doctoral research at PPPL before joining the research staff in 1999. Among his honors, Menard was awarded the Presidential Early Career Award in Science and Engineering in 2004, the "Best Student Paper" award from the American Nuclear Society Fusion Energy Division in 1998, the Princeton University Honorific Fellowship in 1996, and the U.S. Department of Energy Magnetic Fusion Science Fellowship in 1993. The PPPL is funded by the DOE and managed by Princeton University.

DEVELOPMENT OF AN AUTO-CONVERGENT FREE-BOUNDARY AXISYMMETRIC EQUILIBRIUM SOLVER

JONATHAN HUANG, JON MENARD

ABSTRACT

The calculation of the magnetic flux given an assumed value for the current profile in axisymmetric toroidal plasmas is essential in studying the effects of various magnetohydrodynamic (MHD) instabilities upon controlled fusion. To this end, an iterative, modular algorithm coupled with a fast, direct elliptic solver for the Grad-Shafranov equation has been used to reconstruct the desired free-boundary equilibrium solution. This free-boundary Grad-Shafranov (FBGS) equilibrium algorithm is modified with the application of the von Hagenow method for determining the flux on the computational boundary, greatly reducing the time cost from $O(N^3)$ to $O(N^2 \ln N)$ machine operations as compared to current Green's function methods. The inherent variance in implementing the von Hagenow method gives a mean error bound of 0.1 percent with respect to the normal Green's method. The improvements will allow the grid resolution to be increased efficiently and automatically to reduce the maximum Grad-Shafranov error to values needed for accurate stability calculations on a more effective time scale.

INTRODUCTION

The National Spherical Torus Experiment (NSTX) is a medium-sized, low aspect ratio spherical torus (ST) device—a cost-effective, innovative, and compact magnetic confinement concept designed to explore high-beta stability and plasma confinement as a "proof of principle" for controlled fusion. Parameters for the machine are a major radius of R = 0.85 m, minor radius a = 0.67 m, and an aspect ratio R/a = 1.26, with a typical toroidal field B_T < 0.6 T and plasma current of 0.3–1.5 MA.

The shape of the plasma and location of the plasma boundary greatly affect its stability and, therefore, its attractiveness for controlled fusion. Since the electromagnetic fields influence the movement of the plasma which itself induces electromagnetic fields, determining this shape may quickly lead to nonlinear equations. One simple way of studying magnetically confined plasmas with an emphasis on the shaping magnetic field topology is magnetohydrodynamics (MHD), the principle whereby the plasma is treated as a single, electrically-conducting fluid. Certain MHD modes cause alterations in the plasma topology that form magnetic islands, which may lead to large disruptions in a magnetic confinement device. For instance, in NSTX plasmas the 1/1 internal kink mode has been observed to induce energetic ion loss by a factor of 3–5 and cause flattening in the toroidal rotation profile within the plasma core [1].

To understand these and others MHD modes and their resulting impact, it is essential to be able to both accurately predict and reconstruct free-boundary MHD equilibria based on experimental measurements. Moreover, these equilibria are important in reproducing plasma configurations, implementing plasma shape control, and studying the plasma-wall interactions. Equilibria represent the simplest solution to a dynamical system, and thus are a natural starting point. Furthermore, reconstructing sequences of equilibria may be used to model the time evolution of the plasma as a quasi-static approximation.

MHD equilibrium is predicated upon the force balance equation, $\nabla p = \mathbf{J} \times \mathbf{B}$, where p is the pressure, $\mathbf{J}$ the current density,

and **B** the magnetic field. This is the static solution to the ideal MHD equations; it determines the plasma shape and the external fields required for confinement. Noting that from Ampére's Law, $\nabla \times \mathbf{B} = \mu_0 \mathbf{J}$, and from Maxwell's equations, $\nabla \cdot B = 0$, the force balance equation may be simplified in a toroidally symmetric system to the so-called Grad-Shafranov equation. In cylindrical coordinates, this is a non-linear, two-dimensional elliptic partial differential equation whose solution is obtained by a freeboundary Grad-Shafranov (FBGS) algorithm.

In this paper, we present the development of a predictive free-boundary auto-convergent axisymmetric equilibrium solver named ISOLVER. ISOLVER takes normalized pressure and current profiles and boundary shape as input, matches a specified plasma current and β, and computes coil currents as its output. At its core, it contains a modular, iterative algorithm coupled with a fast, direct elliptic solver to the Grad-Shafranov equation. To improve the calculation of the boundary condition for the elliptic equation, the von Hagenow method is implemented. This greatly reduces the time cost of the algorithm, making the time-limiting factor the solution to the differential equation. The grid resolution may be efficiently increased to reduce the maximum Grad-Shafranov error to necessary values for accurate stability calculations. Furthermore, a convergent solution may be calculated once and stored for a given computational grid, and accessed for a particular current profile on a much faster time scale.

In the following section, we shall describe in detail the main FBGS algorithm, including an analysis of the time cost. In Section 3, we shall explain the von Hagenow method, including the nuances of dealing with the inherent logarithmic singularity, and fully describe the significant reduction in time cost. In Section 4 we present a full error analysis of the code, and in Section 5 we shall give concluding remarks and discuss future work.

Main Algorithm

A good example of a FBGS algorithm is the EFIT code which has been used as a freeboundary equilibrium reconstruction technique for many magnetic confinement devices, including DIII-D, JET, and JT-60U. Here we shall describe the main components of codes like EFIT; more rigorous derivations may be found in [2].

The FBGS algorithm solves the Grad-Shafranov equation, which is derived from the force balance equation. Using cylindrical (R, ϕ, Z) coordinates, Maxwell's equations imply that the magnetic field may be expressed as the curl of a vector potential $\mathbf{A} = (A_R, A\phi, A_Z)$. Exploiting of axisymmetric geometry results in the following form for the magnetic field

$$\mathbf{B} = \nabla\phi \times \nabla\Psi(R,Z) + g(R,Z)\nabla\phi \qquad (1)$$

where we define the poloidal flux function $\Psi(R,Z) = -RA_\phi$ and the toroidal field function $g(R,Z) = R(\partial A_R/\partial Z - \partial A_Z/\partial R)$. From Ampére's Law we recognize that the current may be expressed as

$$\mu_0 \mathbf{J} = \Delta^* \Psi \nabla\phi + \nabla g \times \nabla\phi \qquad (2)$$

where we have defined the toroidal elliptic operator as $\Delta^*\Psi \equiv R^2\nabla \cdot (1/R^2)\nabla\Psi$.

Using the axisymmetric forms for the magnetic field from Equation (1) and the current from Equation (2) in the force balance equation, and taking the projection onto the vectors **J** and $\nabla\phi$, we see that p and g are functions of the poloidal flux Ψ. Taking the projection onto the vector $\nabla\Psi$, we obtain the Grad-Shafranov equation $\Delta^*\Psi + \mu_0 R 2p'(\Psi) + gg'(\Psi) = 0$. Equivalently, we may define the toroidal current density $J\phi$ as constructed from the two flux functions $p(\Psi)$ and $gg'(\Psi)$ which are the plasma pressure gradient and the poloidal current functions, respectively, and thus represent the Grad-Shafranov equation as $\Delta^*\Psi = \mu_0 R J_\phi(R,\Psi)$. Hence, an assumed form for the toroidal current profile is dictated by the 3 plasma pressure gradient and the poloidal current functions. In EFIT, these are usually given by a set of basis functions of the normalized flux Ψ_n which are second order polynomials for $p(\Psi)$ and second or third order polynomials for $gg(\Psi)$ [3]. In ISOLVER, $p(\Psi)$ and $\langle \boldsymbol{J} \cdot \boldsymbol{B} \rangle(\Psi)/\langle B \cdot \nabla\phi \rangle$ are the specified profiles and the sound-speed Mach number $M_S(\Psi)$ is also specified to include the effects of plasma rotation on the equilibrium.

The Grad-Shafronov equation given in cylindrical coordinates,

$$R\frac{\partial}{\partial R}\frac{1}{R}\frac{\partial\Psi}{\partial R} + \frac{\partial^2\Psi}{\partial Z^2} = \mu_0 R J_\phi R J\phi(R,\Psi) \qquad (3)$$

is a separable elliptic partial differential equation. This may be handled by using Fast Fourier Transform techniques or applying the generalized Buneman Algorithm. A consistent solution to the elliptic equation is found by iterating on the Ψ dependence in the source function $\mathbf{J}_\phi(R,\Psi)$ with a Picard iteration technique, $\Delta^*\Psi^{n+1} = \mu_0 R J\phi(R,\Psi^n)$. The iteration is kept convergent by altering $J\phi$ through the free functions $p(\Psi)$ and $g(\Psi)$ to meet the specified constants.

In order to solve Equation (3), the flux along the computational boundary must be provided as a boundary condition for the elliptic solver. To determine the boundary flux given the plasma toroidal current density and the current Ic measured in conductors located outside the plasma boundary at positions (R^i_c, Z^i_c), we employ the Green's function for the differential operator $\Delta^*\Psi$,

$$G(R,R') = \frac{\mu_0}{2\pi}\frac{\sqrt{RR'}}{k}[(2-k^2)K(k^2) - E(k^2)] \qquad (4)$$

$$\text{where the argument } k2 = \frac{4RR'}{(R+R')^2 + (Z-Z')^2}$$

and $K(k^2)$ and $E(k^2)$ are the complete elliptic integrals of the first and second kind, respectively. The Green's function by definition satisfies $\Delta^*G(\mathbf{R},\mathbf{R}') = \delta(\mathbf{R}-\mathbf{R}') = R\delta(\mathbf{R}-\mathbf{R}')\delta(Z-Z')$ and the flux function satisfies

$$\Delta^*\psi(R) = \mu_0 R J\phi(R) = \mu_0 R J\phi(R,Z) \text{ in plasma}$$
$$= \mu_0 \Sigma\, RIi\delta(R-R^c_i)\delta(Z-Z^c_i) \text{ in vacuum}$$

where Nc is the total number of coils, and (R^c_i, Z^c_i) is the position of and I_i the current in the ith coil.

In order to use these relations to solve for the boundary flux, first consider the following vector identity applied to Ψ and G,

$$\nabla \cdot \left(\Psi\frac{1}{R^2}\nabla G - G\frac{1}{R^2}\nabla\Psi\right) = \Psi\frac{\Delta^*G}{R^2} - G\frac{\Delta^*\Psi}{R^2} \qquad (5)$$

Letting the observation point (R', Z') lie on the computational boundary, integrate Equation (5) over all space. Using the Divergence Theorem, the left hand side reduces to surface integrals which vanish

at infinity. After integration, the first term on the right hand side becomes the boundary flux. Integration over the second term on the right hand side may be broken into integrating over the plasma and the vacuum. Hence, we have for the flux boundary

$$\begin{aligned}\Psi_b(R',Z') &= \int_{\text{plasma}} G(\mathbf{R};\mathbf{R}')\frac{\Delta^*\Psi(\mathbf{R})}{R^2} + \int_{\text{vacuum}} G(\mathbf{R};\mathbf{R}')\frac{\Delta^*\Psi(\mathbf{R})}{R^2} \\ &= \mu_0 \int_{\text{plasma}} G(\mathbf{R},\mathbf{R}')J_\phi(\mathbf{R})\,dR\,dZ + \mu_0 \sum_{i=1}^{N_c} G(R_i^c, Z_i^c; R', Z')I_i \qquad (6)\end{aligned}$$

In summary, a FBGS algorithm takes an initial guess for the toroidal current profile J_{ϕ} and executes an iterative technique to compute a convergent flux solution. Once given a boundary condition flux, the algorithm solves Equation (3) using a fast direct method for elliptic equations. Inverted, the elliptic equation has the following finite difference form

$$\begin{aligned}&\frac{R_i}{\Delta R^2}\left[\frac{1}{R_{i+1/2}}\left(\Psi_{i+1,j}^{n+1} - \Psi_{i,j}^{n+1}\right) - \frac{1}{R_{i-1/2}}\left(\Psi_{i,j}^{n+1} - \Psi_{i-1,j}^{n=1}\right)\right] \\ &\quad + \frac{1}{\Delta Z^2}\left[\Psi_{i,j+1}^{n+1} - 2\Psi_{i,j+1}^{n+1} + \Psi_{i,j+1}^{n+1}\right] = \mu_0 R_i J_{\phi i,j}^n \qquad (7)\end{aligned}$$

A Fast Fourier Transform technique would require N transforms for $J_{\phi ij}$, where N is the number of grid points in the Z direction (index j), each requiring $O(N\ln N)$ operations. After solving the $5M$ tri-diagonal equations where M is the number of grid points in the R direction (index i), another N transforms are required to bring the solution back into $\Psi_{i,j}$. In total, the number of operations required to solve the elliptic equation is $O(N^2 \ln N)$.

To arrive at a boundary solution, the integral in Equation (6) must be evaluated. The two dimensional integral becomes a double sum over R and Z, which can be expensive to evaluate. Assuming there are N grid points in each direction, to evaluate this sum requires $O(4N^3)$ operations, and determining the flux on the computational boundary can become the limiting factor in the FBGS algorithm. The algorithm iterates the boundary flux computation through the current profile given by a consistent flux solution until the boundary flux and other profiles converge

Von Hagenow Method

The von Hagenow Method[4] is a technique used to greatly reduce the time cost in calculating the boundary flux Ψ_b. Namely, it implements a new method of evaluating the costly integral in Equation (6).

First, consider a psuedo-flux function $U(R,Z)$ that satisfies the same elliptic equation as Ψ but is canonically 0 on the boundary. Then, applying the same vector identity as in Equation (5) now to U and G, we have that

$$G\frac{\Delta^* U}{R^2} = U\frac{\Delta^* G}{R^2} - \nabla\cdot\left(U\frac{\nabla G}{R^2}\right) + \nabla\cdot\left(G\frac{\nabla U}{R^2}\right) \qquad (8)$$

where we choose the observation (R',Z') to be a small distance outside the computational boundary, and we take the limit as $\epsilon \to 0$.

Integrating the expression in Equation (8) over the computational domain, and using the relations for $\Delta^* U$, the term on the left hand side becomes the sought-after integral in Equation (8). Noting the behavior of U on the boundary, the integral of the first term on the right hand side vanishes, and so does the second term after application of the divergence theorem. Thus, we arrive at the following expression for the desired integral

$$\mu_0 \int_{\text{plasma}} G(\mathbf{R},\mathbf{R}')J_\phi(\mathbf{R})\,d\mathbf{R} = \int_{\text{boundary}} \frac{G(\mathbf{R},\mathbf{R}')}{R}\frac{\partial U}{\partial n}\,d\ell \qquad (9)$$

This line integral around the boundary is much cheaper to evaluate than the whole integral over the computational domain. First, the inherent symmetries in the Green's function for the toroidal elliptic operator reduce the number of total evaluations needed. Noting closely the form in Equation (4), we see that $G(\mathbf{R},\mathbf{R}')$ is symmetric in its arguments and is only dependent on the three variables R, R', and $(Z - Z')^2$. These symmetries reduce the number of calculations of the Greens function from $16N^2$ to close to $3N^2$ machine operations. The solution to the psuedo-flux U may be found using similar fast direct methods as for the original flux, which takes $O(N^2 \ln N)$ as previously discussed. The derivative may be easily and accurately approximated by analytically differentiating a three-point bicubic spline interpolation. Thus, the time limiting factor has been reduced to solving the elliptic equation.

The problem that arises using this method to compute the boundary flux is the behavior of the Green's function $G(\mathbf{R},\mathbf{R}')$ at the point $(R,Z) = (R',Z')$. The boundary integral that we seek to evaluate given by Equation (9) has a logarithmic singularity which can be removed analytically. The Green's function term behaves like

$$g(\mathbf{R},\mathbf{R}') \equiv \frac{G(\mathbf{R},\mathbf{R}')}{R} \simeq -\frac{1}{4\pi}\ln\left(\frac{\ell - \ell_0}{2R_0}\right)^2 \qquad (10)$$

with a singularity at the boundary $\ell = \ell_0$, where we have parameterized $\mathbf{R} = \mathbf{R}(\ell)$ and $\mathbf{R}' = \mathbf{R}(\ell_0)$

The removal of the logarithmic singularity may be dealt with in several ways, the most accurate and straightforward of which is to express the derivative as $\partial U/\partial n$ = constant + $\partial U'/\partial n$ where the variable term $\partial U'/\partial n$ vanishes at the singularity. Thus, we may analytically evaluate the singular behavior of the Green's function term $g(\mathbf{R},\mathbf{R}')$ around the boundary and numerically integrate the remaining terms which are no longer exhibit singularities.

Specifically, to evaluate the integral at the boundary point given by ℓ_0, we first express the derivative as

$$\frac{\partial U(\ell)}{\partial n} = \frac{\partial U(\ell_0)}{\partial n} + \left(\frac{\partial U(\ell)}{\partial n} - \frac{\partial U(\ell_0)}{\partial n}\right) \qquad (11)$$

And the total Green's function term is broken into its singular component $gs(\boldsymbol{\ell})$ given by Equation (10) and non-singular component $gns(\boldsymbol{\ell})$ which is determined by simply subtracting out the singular component from the total. Thus the line integral may treated by three separate integrands,

$$\int g(\ell)\left(\frac{\partial U(\ell)}{\partial n} - \frac{\partial U(\ell_0)}{\partial n}\right)d\ell + \frac{\partial U(\ell_0)}{\partial n}\int g_s(\ell)d\ell + \frac{\partial U(\ell_0)}{\partial n}\int g_{ns}(\ell)d\ell \qquad (12)$$

The first integral no longer has a singularity due to the behavior of the variable derivative term, and the third integral is easily evaluated. The second integral may be determined analytically.

RESULTS

In the implementation used for the following results, we have used for computational convenience a simpler approximation to the integration through the logarithmic singularity. Instead of the method described in Section 3, we simply treat the singularity locally at the two points closest to the singularity, replacing the entire Green's function term by the singular approximation and ignoring the non-singular part. Though less accurate, this calculation remains viable since the local contribution missing from the non-singular term at the singularity is almost negligible around the whole boundary. The mean relative contribution is 0.00035, decreasing the computed boundary flux result from its actual value.

Figure (1) shows the entire computed boundary solution plotted linearly for the von Hagenow method (plotted in black) and the slower summing Green's function method (plotted in red). Figure (2) shows a closer comparison at each side of the computational boundary. The maximum error against the Green's method calculated boundary values was observed to be 0.00019 for the bottom, 0.00196 for the right, 0.00022 for the top, and 0.00016 for the left, with respective mean relative errors of 0.02326, 0.02326, 0.00301, and 0.00598. Figure (3) shows the ratio of the regular computed value over the von Hagenow computed value. Figure (4) shows the inherent computational variance in the von Hagenow and Green computed boundary, and the ratio of disagreement. The inherent mean relative error is 0.00174.

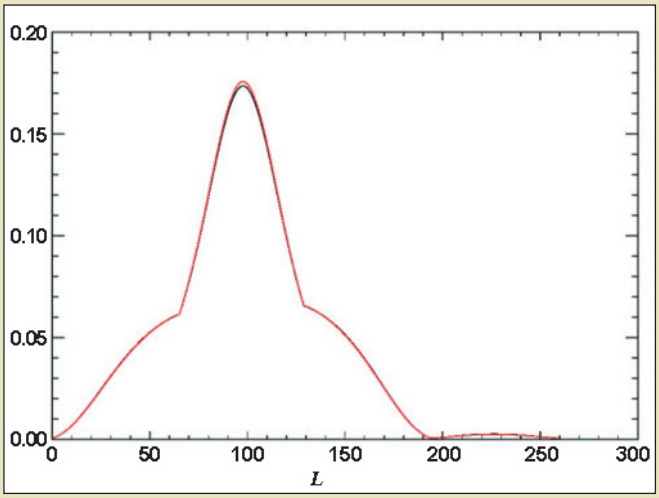

Figure 1. Linear plot of the entire boundary solution with and without von Hagenow implementation

Figure (5) contains contour plots of the equilibrium flux computed using the von Hagenow and the Green's method to compute the boundary flux.

A more exact application of the von Hagenow method should differ from the normal Green's method by a limiting inherent relative error of 0.1 percent. However, it is clear from Figure (2) that the error in the bottom and right side of the boundary are off by an order of magnitude, which is larger than expected from ignoring the local contribution of the non-singular Green's term to the boundary flux. These systematic errors affect the entire equilibrium solution. Furthermore, the behavior of the error and ratios at the corners of the boundary are not consistent with the fact that the approximation of the pseudo-flux derivative $\partial U/\partial n$ is canonically set to vanish at the corner values. This points at possible minor errors in the specific application of the von Hagenow method and treatment of the Green's function term at the singularity.

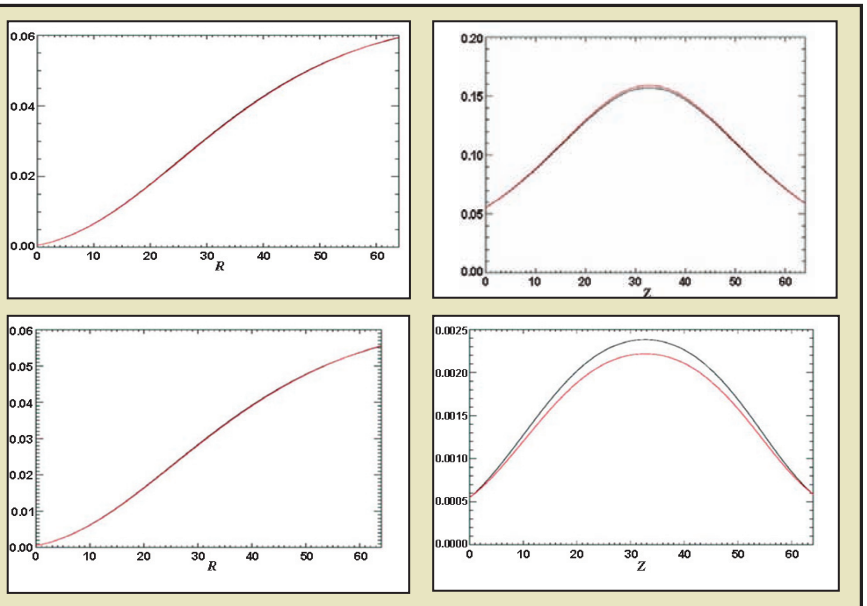

Figure 2. Plots of the boundary flux.

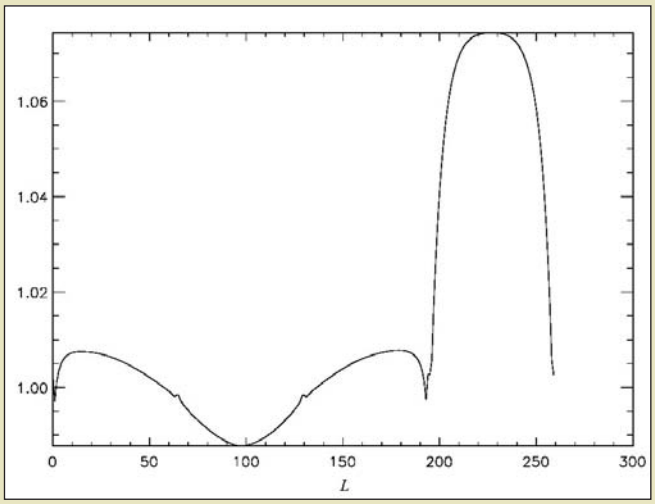

Figure 3. Ratio of von Hagenow computed value versus normal value.

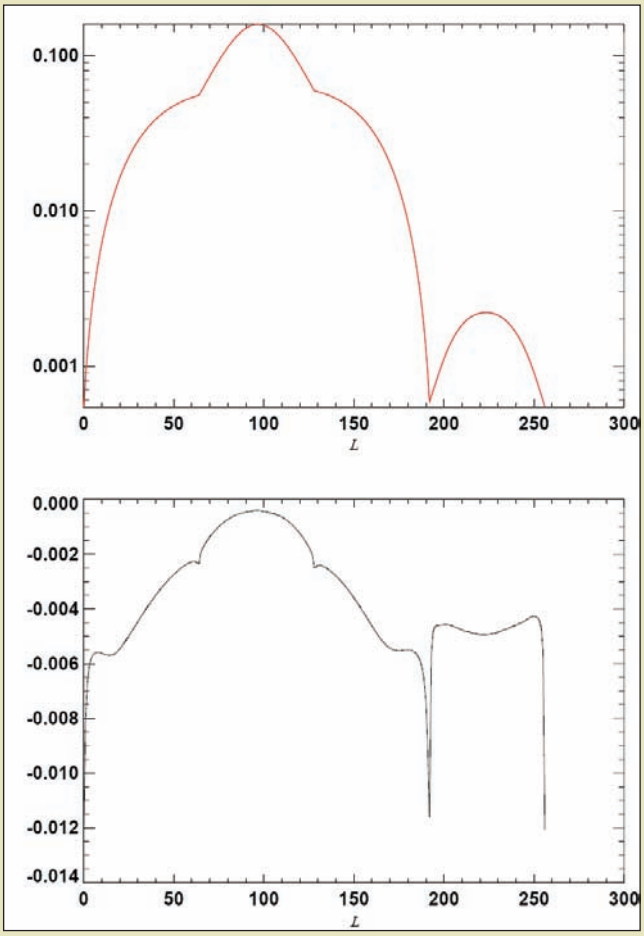

Figure 4. Inherent variance in von Hagenow method and ratio.

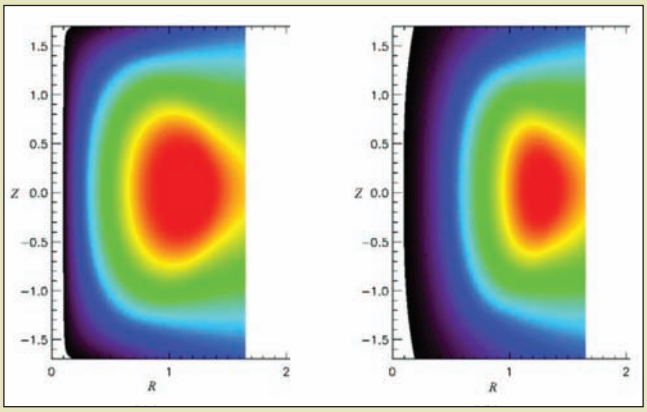

5(a) Contour plot of Ψ using von Hagenow method

5(b) Contour plot of Ψ using normal Green's method

Figure 5. Contour plots of the equilibrium flux.

DISCUSSION AND CONCLUSIONS

A sufficiently accurate application of the von Hagenow method in a modified implementation of the FBGS algorithm has been accomplished. The costly computation of the boundary flux has been greatly reduced so that the limiting factor in the total equilibrium algorithm becomes the solution of the differential equation, which may be handled using fast direct elliptic methods. The total time cost reduces from $O(N4)$ to $O(N^2 \ln N)$.

Future studies should investigate the behavior of the Green's function term at the corner boundary values, and reduce the disagreement in the von Hagenow method to below 0.1 percent. Furthermore, the method should be implemented to create a more modular FBGS algorithm, computing the necessary values once for a given grid resolution, which may be changed efficiently to reduce the maximum Grad-Shafranov error. The improved FBGS algorithm may be implemented within ISOLVER, which computes free-boundary equilibria.

ACKNOWLEDGEMENTS

The author would like to thank Dr. J. Menard for his guidance throughout this project and many helpful discussions and Mr. J. Morgan for his support. The work was completed within the Science Undergraduate Laboratory Internship program in the Office of Science of the U. S. Department of Energy under DE-AC02-76CH0307.

REFERENCES

[1] J. E. Menard, R. E. Bell, E. D. Fredrickson, et al., "Internal kink mode dynamics in high-beta nstx plasmas," *Nucl. Fus.,* vol. 45, pp. 539–556, 2005.

[2] L. L. Lao, H. St. John, R. D. Stambaugh, et al., "Reconstruction of current profile parameters and plasma shapes in tokamaks," *Nucl. Fus.,* vol. 25, no. 11, p. 1611, 1985.

[3] S. A. Sabbagh, S. M. Kaye, J. Menard, et al., "Equilibrium properties of spherical torus plasmas in nstx," *Nucl. Fus.,* vol. 41, no. 11, p. 1601, 2001.

[4] S. C. Jardin, N. Pomphrey, and J. Delucia, "Dynamic modeling of transport and positional control of tokamaks," *Journal of Comp. Phys.,* vol. 66, no. 2, pp. 481–507, 1986.